JOURNAL OF CATALYSIS 141, 206–218 (1993)

Characterization of Tungsten-Modified Ultrastable Y Zeolite Catalysts and Their Activity in Thiophene Hydrodesulfurization

R. CID,* J. NEIRA,* J. GODOY,* J. M. PALACIOS,† S. MENDIOROZ,† AND A. LÓPEZ AGUDO†

*Departamento de Química, Facultad de Ciencias, Universidad de Concepción, Casilla 3-C, Concepción, Chile; and †Instituto de Catálisis y Petroleoquímica, C.S.I.C., Serrano 119, 28006-Madrid, Spain

Received June 17, 1991; revised September 24, 1992

Tungsten-modified ultrastable Y (USY) zeolite catalysts, prepared by conventional impregnation with ammonium metatungstate solutions at three different pHs and calcined at 350, 450, and 550°C have been characterized by X-ray diffraction (XRD), infrared spectroscopy (IR), scanning electron microscopy–energy dispersive X-ray analysis (SEM–EDX), and acidity and surface area measurements. They have also been evaluated for hydrodesulfurization (HDS) of thiophene and subsequent hydrogenation (HYD) of butenes in both oxidic and sulfided states. The incorporation of tungstate ions in the USY followed by calcination at high temperature was found to cause a small loss of crystallinity, particularly for the catalysts impregnated at acidic pH. In this case, the EDX and N_2 adsorption results indicated that most of tungsten was inhomogeneously deposited outside the zeolite cavities, but without forming WO_3 species that could be detected by XRD. This location of tungsten and the increased acidity after sulfidation with H_2S generated a substantial increase in HDS activity relative to the parent USY, and the appearance of HYD activity. Conversely, in the catalysts prepared at basic pH, a large part of the tungsten is inside the zeolite cavities, most probably in the supercages. This tungsten location and the loss of acidity resulted in a very low HDS activity and no HYD activity for both calcined and sulfided catalysts.

INTRODUCTION

In recent years great efforts have been made to develop new hydrocracking catalysts having increased activity for hydrodesulfurization (HDS) and hydrodenitrogenation (HDN) reactions in order to satisfy the needs of processing low-quality crude oil. In these catalysts the cracking functionality is mainly provided by a zeolitic component and the hydrogenation (HYD) one by sulfided tungsten (or molybdenum) promoted with nickel (*1–5*). The tungsten is generally added to the crystalline component (zeolite) by the same method as used for amorphous catalyst supports (alumina, silica–alumina), viz., by impregnating the zeolite with ammonium tungstate solutions.

Since impregnation is not a simple process, it is expected that, as occurs for the conventional alumina-supported tungsten or molybdenum hydrotreating catalysts, the procedure and conditions used for the preparation of zeolite-based tungsten catalysts will also significantly affect the catalyst surface, and therefore its catalytic properties. The preparation of tungsten-based catalysts by impregnation is known to be complicated by the possible presence of different tungstate species in solution. However, studies on zeolite-based tungsten catalysts are very scarce in the scientific literature, the majority concerning the activity and selectivity of hydrocracking of polycyclic aromatic feeds (*4*) and quinoline HDN (*5*). The effect of the pH of the impregnation solution on the location of WO_3 in extrudates of WO_3/Y zeolite and their catalytic behaviour for 1-hexene cracking have been reported only recently (*6*). No effects of either impregnation pH or calcination temperature on the crystallinity of the zeolite were revealed.

0021-9517/93 $5.00

Previous studies on molybdate-impregnated Y zeolite catalysts showed, however, that both Mo loading and calcination conditions caused changes in the zeolite structure (*7*) and that the thermal treatment affected the location of Mo ions in the zeolite (*8, 9*).

In the present work we examine the influence of the impregnation pH and subsequent calcination temperature on the surface structure and activity for thiophene hydroconversion of WO_3/USY zeolite catalysts. This could be helpful for understanding the catalytic behaviour of more complex catalysts in hydrocracking processes.

EXPERIMENTAL

Catalyst Preparation

UltrastableY (USY) zeolite was prepared by repeated sodium exchange of zeolite NaY (Linde LZ-Y52), Si/Al = 2.5, with aqueous solutions of NH_4NO_3 at 35°C for 12 h followed by steaming at 650°C for 3 h. The USY zeolite sample obtained had a Si/Al ratio of 3.5 and 30% of extra framework Al species.

Catalysts with 10 wt% WO_3 were prepared by impregnation of the USY zeolite with aqueous solutions of ammonium *meta*-tungstate (AMT) at three different pH values: 2.7, 5.6, and 11. The pH was adjusted to the appropriate value by adding HNO_3 or NaOH solution. The zeolite/solution volume ratio was $\frac{1}{6}$. Complete elimination of water was performed in a rotary evaporator by heating at 36°C under reduced pressure for 3 h. The impregnated samples were dried at 110°C and then divided into three portions, which were calcined at different temperatures (350, 450, or 550°C, respectively) in air for 4.5 h. The catalysts are denoted as W-$x(T)$, where x is the pH of impregnation and T the final calcination temperature, i.e., W-5.6(550) means that the WO_3/USY catalyst was prepared at pH 5.6 and calcined at 550°C.

Additional reference catalysts were prepared as follows. The catalyst designated USY-11 was a sample of USY treated with NaOH solution at pH 11 for 3 h, then dried in a rotary evaporator and finally calcined at 550°C for 4.5 h. The catalyst denoted as W-2.7(550)-E was a W-2.7(550) sample leached with dilute ammonia solution (*9*) to extract partially the WO_3, then filtered, and calcined also at 550°C for 4.5 h. A mechanical mixture of USY and 10 wt% WO_3 was prepared by ultrasonic dispersion in isopropanol solution; it was dried and calcined as for the previously leached catalyst. The catalysts studied are listed in Table 1.

Physicochemical Characterization

The surface area (S_{BET}) of the catalysts was determined by nitrogen adsorption (BET method) at −196°C in an ASAP 2000 apparatus from Micromeritics Instrument Co. The p/p_0 range used for the BET plot was 0.005–0.1. In all cases correlation coefficients higher than 0.999 were obtained. The N_2 adsorption–desorption isotherms of some representative catalysts were independently performed using the same apparatus. The samples were pretreated at 140°C for 18 h under vacuum (10^{-5} Torr) before isotherm acquisition.

X-ray diffraction (XRD) measurements were made with a Philips PW Diffractometer using Ni-filtered Cu $K\alpha$ radiation. Unit cell size was determined by ASTM procedure 3942-80 using Si as an internal standard. The estimated standard deviation was ±0.02 Å. The degree of X-ray crystallinity was estimated from the intensities of five major reflections in the region 2θ = 10°–45° relative to the original USY zeolite calcined at comparable temperature. Signal attenuation by tungsten was not corrected for.

A Nicolet ZDX Fourier Transform infrared (FTIR) spectrometer was used to obtain spectra in the skeletal vibration region (1400–400 cm^{-1}) using the conventional KBr disk technique. The absorbance ratio of the bands at 591 and 457 cm^{-1} is used as a parameter to estimate the crystallinity of zeolites (*10*).

Scanning electron microscopy (SEM) and energy dispersive X-ray (EDX) microanalysis were carried out in an ISI DS-130 micro-

TABLE 1

Physical Properties of the Samples

Catalyst	Surface area ($m^2\ g^{-1}$)[a]	Crystallinity (%)		Unit cell parameter a_0 (Å)
		XRD	IR[b]	
USY zeolite	717	100	100	24.52
W-2.7(350)	532	66	108	—
W-2.7(450)	628	50	111	—
W-2.7(550)	632	60	97	24.48
W-5.6(350)	598	68	—	—
W-5.6(450)	612	90	—	—
W-5.6(550)	625	87	97	24.50
W-11(350)	144	81	—	—
W-11(450)	258	60	—	—
W-11(550)	298	79	110	24.57
W-2.7(550)-E	333	—	—	—
USY + 10 wt% WO_3	575	88	—	—
USY-11	870	118	—	24.60

[a] The 0.005–0.1 p/p_0 range was used.

[b] Based on the intensity ratio of the bands at 591 and 457 cm^{-1} relative to that for the USY.

scope equipped with a Si/Li detector and a Kevex 8000-II processor. The samples for morphological study were coated with a gold film, and those for analytical study were pressed into wafers and then coated with a carbon film.

Surface acidity of catalysts was measured potentiometrically by titration with *n*-butylamine in acetonitrile using an Ag/AgCl electrode. The details of the experimental procedure are described elsewhere (*11*).

Evaluation of Catalytic Activity

Hydroconversion of thiophene was performed in a flow microreactor operating at atmospheric pressure. Thiophene was fed (11.8×10^{-8} mol min^{-1}) by bubbling H_2 (40 ml min^{-1}) through a bubbler containing liquid thiophene at 0°C. The catalyst (300 mg, particle size 25-35 mesh ASTM) was packed in the reactor and presulfided with a mixture of 5 vol% of H_2S in H_2 at 400°C for 3 h. Samples of the effluent gas were analyzed with an on-line gas chromatograph, using a 3 m × $\frac{1}{8}$ in. O.D. column of *n*-octane Porasil C. Because most catalysts suffered deactivation, reaction was followed for about 3.5 h, when the activity had decreased to a more or less constant level. Thiophene conversion was calculated from the ratio converted thiophene/initial thiophene; coked thiophene, therefore, was included in this calculation. Coke deposited on the catalysts was not determined. The pseudo-first-order rate constant for HDS (k_{HDS}) was calculated at different reaction times by the equation: $k_{HDS} = F/W\ (\ln 1/(1 - x))$, where W is catalyst weight, F is the feed rate of thiophene, and x is the fractional conversion. The selectivity for hydrogenation (HYD) of butenes to butane, expressed as the ratio k_{HYD}/k_{HDS}, was calculated according to the method of Okamoto *et al.* (*12*).

RESULTS AND DISCUSSION

Effect of Tungsten Incorporation on Zeolite Structure and Tungsten Location

The unit cell size of the sample USY was 24.52 Å.

All X-ray diffraction peaks appearing in

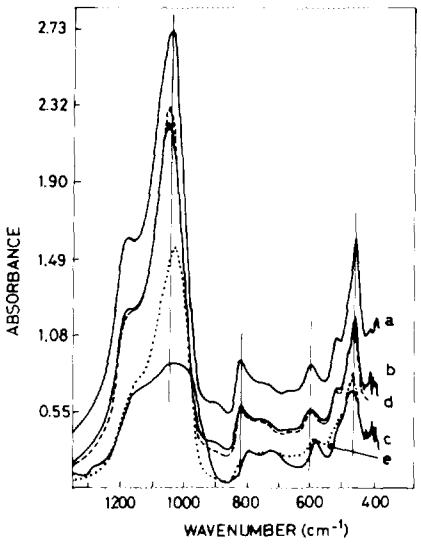

FIG. 1. Infrared spectra of catalysts (a) W-2.7(550), (b) W-5.6(550), (c) W-11(550), (d) parent USY, and (e) mechanical mixture 1 : 1 of USY and NaY zeolites.

the diffractogram of the starting USY zeolite were also present in the patterns of the W-loaded USY catalysts, but remarkable variations in the relative intensity of some peaks were observed. Peaks different from those of the USY zeolite were, however, not detected in any W-loaded catalyst, irrespective of the calcination temperature. Moreover, no increase in the background due to amorphous material was observed. The peak intensities of the catalysts were generally lower than those of the USY zeolite, except for the W-11 samples in which the peaks with *d*-spacings of 5.35, 3.26, and 2.77 Å were more intense. Since these peaks did not coincide with the major ones of WO_3, viz., at 3.84, 3.76, 3.65, and 2.62 Å, WO_3 if present, would be amorphous and/or small grained.

On the other hand, the IR spectra (see Fig. 1) can neither prove the presence or absence of a WO_3 phase since this compound exhibits a broad band with maximum at ca. 814 cm^{-1}, which is very close to the symmetric external stretching vibration of TO_4 tetrahedra of the USY zeolite.

We relate the observed increase in intensity of the above XRD peaks of the W-11 samples to a redistribution of Na^+ ions and/or alumination changes rather than to a distortion of the structure caused by interaction of the tungstate anions with the zeolite framework. Changes in framework Al are suggested by comparing the unit cell parameter, a_0, found for the catalysts (Table 1). Thus, the catalyst preparation at pH 2.7, followed by calcination at 550°C, had a small decrease (0.16%) in the unit cell parameter relative to the USY zeolite, which suggests a slight shrinkage of the framework by further dealumination, caused possibly by the acid medium (*13*) during impregnation and subsequent thermal treatment. On the contrary, the catalyst preparation at pH 11 led to a significant increase (0.20%) in the unit cell parameter, indicating framework realumination (*14*), which may be caused by the NaOH addition (*15–18*) to adjust the impregnation pH to 11 during the preparation.

Further support for this conclusion comes from the IR results (Fig. 1 and Table 2). For the W-5.6(550) and W-2.7(550) catalysts, the position of their bands practically did not change or shifted only slightly towards higher wavenumbers in comparison with the parent USY zeolite. In contrast, all the bands of the W-11(550) catalyst, except that at ca. 457 cm^{-1} (corresponding to T–O bending) which is insensitive to framework composition (*19*), were generally less intense and sharp, and shifted significantly towards lower wavenumbers with respect to the USY zeolite. This decrease in intensity and sharpness, and general shift of the bands, indicate some loss of crystallinity and that Al has been reinserted into the zeolitic framework (*14–17*). Such realumination is also proved by comparing the band positions of the W-11(550) catalyst with those of the mechanical mixture USY ± NaY (Table 2). In addition, the band at ca. 724 cm^{-1}, relative to the symmetric Si–O–Al, was relatively more intense in the W-11(550) catalyst than in the USY zeolite. These changes are consistent with the observed increase in the unit cell parameter.

TABLE 2

Position of the Infrared Vibrational Frequencies of the W-Modified Ultrastable Zeolite Catalysts Calcined at 550°C

Catalyst	Asymmetric stretch (cm^{-1})		Symmetric stretch (cm^{-1})		Bending (cm^{-1})		
USY zeolite	1172	1050	814	~735	591	513	457
W-2.7(350)	1172	1050	815	~740	594	512	455
W-2.7(450)	1171	1053	815	~735	591	511	457
W-2.7(550)	1177	1050	818	~732	596	514	455
W-5.6(550)	1172	1052	818	~735	593	513	457
W-11(550)	1140	1028	791	~724	578	507	456
USY + NaY[a]	1148	1030	788	~726	577	507	452

[a] Mechanical mixture, approximately 1 : 1.

Figure 2 shows the spectra of the W-2.7 catalysts calcined at different temperatures. Calcination did not modify qualitatively the spectrum, affecting only the intensity and sharpness of the bands which increased markedly after calcination at 550°C, indicating a higher degree of ordering of the framework. Similar behaviour with calcination temperature was observed for the other catalysts prepared at pH 5.6 and 11.

The data of Table 1 indicate that X-ray crystallinity decreased apparently by ca. 40, 15, and 20% for the 550°C-calcined W-2.7, W-5.6, and W-11 catalysts, respectively, in comparison with that of the parent USY zeolite. For the 350°C- and 450°C-calcined catalysts the losses of crystallinity were roughly similar to those of 550°C-calcined catalysts. This partial breakage of the crystal structure, apparently larger for the catalysts prepared at pH 2.7 (and also for the most acid catalyst; see Table 5), is due to the interaction of tungstate anions with the zeolite framework, which seems to be favoured by the acidic hydroxyl groups of the zeolite, as was also found for Mo-containing Y zeolite catalysts prepared also by impregnation (*8, 9, 20*). These losses in X-ray crystallinity were not, however, parallel to those estimated from IR results (Table 1) which, as found in other studies (*8, 21, 22*) were lower than those obtained from XRD, due in part to X-ray absorption by the W and also to the higher sensitivity of XRD to long range order. The variation in crystallinity as estimated by FTIR was ±10% for all catalysts. In line with this, the surface area losses of the W-2.7 and W-5.6 catalysts calcined at 550 and 450°C, in comparison with the parent USY zeolite, were about 12–15%; and for the corresponding samples calcined at 350°C the losses were higher, about 26 and 16%, probably due to an in-

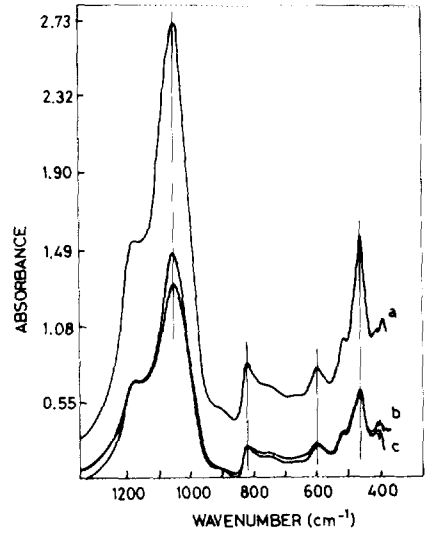

FIG. 2. Infrared spectra of the sample W-2.7 calcined at (a) 550°C, (b) 450°C, and (c) 350°C.

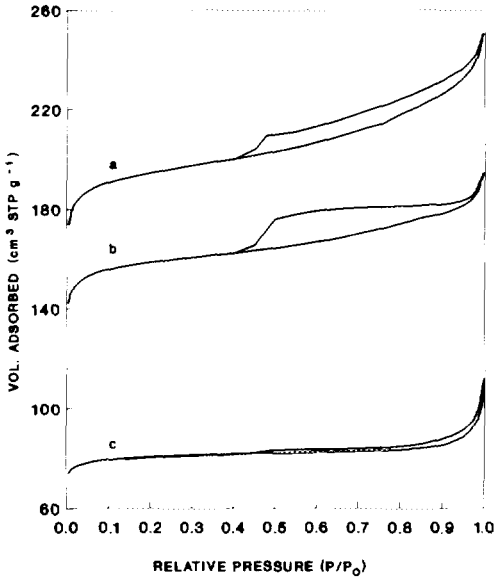

FIG. 3. Adsorption-desorption isotherms for N_2 at −196°C on samples (a) USY, (b) W-2.7(450), and (c) W-11(450).

complete dehydration of the samples and partial blockage of pores by undecomposed bulky tungstate species at such a low calcination temperature. However, for the W-11 catalysts, the losses of surface area were apparently very high: 58% for the sample calcined at 550°C, and 78% for that calcined at 350°C. This contrasts with the relatively high crystallinity, according to both XRD and IR results, that the W-11 samples maintained. This apparent discrepancy suggests that the observed marked decrease in their surface area is mainly associated with a decrease of the sorption capacity by partial occupation of the interior of the zeolite cavities and/or blockage of their access by tungstate anions (at low calcination temperature) and WO_3-like species (at high calcination temperature).

Further light on these two possibilities comes from the comparison of the N_2 adsorption–desorption isotherms shown in Fig. 3 and the data calculated from them, given in Table 3. Tungsten incorporation at acid and basic pH clearly decreased sorption capacity of the USY zeolite, and also changed the shape and the extent of the hysteresis loop which is generally exhibited by dealuminated zeolites (*23, 24*). The USY zeolite presented a typical H4 hysteresis loop (*25*), corresponding to a microporous sample having also a slightly developed slit-shaped interparticulate mesoporosity, as in a face-to-face arrangement of crystalline materials. The W-2.7(450) catalyst presented an apparently more developed hysteresis loop. The desorption branch of this isotherm, with almost no N_2 desorption in the 0.9–0.5 p/p_0 range, is more alike to a type H2 (formerly type E) hysteresis, obtained with "ink-bottle" pores; the adsorption branch suggests a more rigid system than the expandable one described above for the USY zeolite. Furthermore, it is noted that the mesopore size distribution, as deduced from numerical analysis of the adsorption data by the Barret–Joyner–Halenda (BJH) method (*26*), is the same for both catalysts (see Fig. 4). These textural

TABLE 3

Pore Volumes and Average Pore Diameter from N_2 Adsorption Isotherms

Sample	Micropore volume ($cm^3\ g^{-1}$)	Total pore volume ($cm^3\ g^{-1}$)	Average pore diameter (Å)
USY	0.265	0.374	21
W-2.7(450)	0.219	0.290	21
W-11(450)	0.115	0.157	18 24

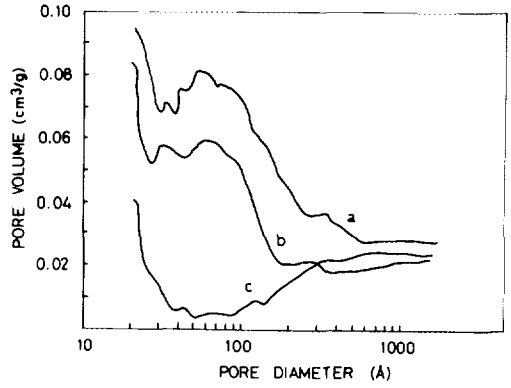

FIG. 4. Pore volume distribution for samples (a) USY, (b) W-2.7(450), and (c) W-11(450).

characteristics of the W-2.7(450) catalyst suggest then that a layer of tungstate may be deposited on the catalyst surface, causing a random aggregation of the particles and then giving rise to ink-bottle porosity. In contrast with this, for the W-11(450) catalyst the hysteresis loop was almost undetectable and appeared to be of the H4 type, as for the USY zeolite, and the total pore volume had about half the value of the two other catalysts. Both microporosity (Table 3) and mesoporosity below 200 Å pore size (Fig. 4) of the W-11(450) sample underwent an important decrease as compared with the two other catalysts. This marked difference in porosity and, consequently, in surface area among the catalysts indicates that in the W-11(450) catalyst (and probably also in the 550°C-calcined one) a substantial part of its void volume is occupied by tungstate, filling up or blocking the micropores corresponding to the zeolite supercages.

The SEM–EDX results provided more insight into the homogeneity of the tungsten distribution and its location in the zeolite. Direct examination at high magnification of the 550°C-calcined catalysts did not reveal substantial differences in particle size (0.5–1 μm) and morphology between the starting USY zeolite and the W-loaded catalysts which could suggest the presence of any WO_3 particle. Only crystals and agglomerates with the characteristic polyhedral shape of Y-type zeolite were observed. This observation is consistent with the XRD and IR results. However, the EDX spectra revealed that catalysts differed significantly in the W $L\alpha$ and $L\beta$ line intensities, as Fig. 5 illustrates. The W $M\alpha$ main lines cannot be used because they overlap those of Si $K\alpha$. Table 4 shows semiquantitative values of the average WO_3 content of a surface area of ca. 1 cm^2 for 550°C-calcined W-loaded catalysts, and the standard deviation (σ) corresponding to the microanalysis of five randomly selected spots (ca. 1 μm^2), which gives information on the tungsten dispersion. Although these values may have a cer-

TABLE 4

Average WO_3 Content Determined by SEM–EDX

Catalyst	Average WO_3[a] content (wt%)	Standard deviation, σ (wt%)
W-2.7(550)	9.2	1.7
W-5.6(550)	11.9	5.5
W-11(550)	1.2	0.4

[a] Calculated from W L_α X-ray line intensity.

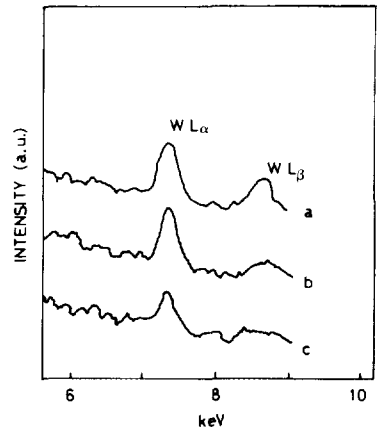

FIG. 5. SEM–EDX spectra in the region 6–10 keV for catalysts (a) W-2.7(550), (b) W-5.6(550), and (c) W-11(550).

tain error by the strong overlapping of the Si $K\alpha$ and W $M\alpha$ lines, they nevertheless allow one to make a relative comparison of the W distribution on the catalysts. It is interesting that the EDX average W contents measured for the W-2.7(550) and W-5.6(550) catalysts were very similar to, and slightly higher than, respectively, the nominal W composition, but their σ values were considerably high. By contrast, the EDX average WO_3 content of the W-11(550) catalyst was extremely low (ca. 1%) in comparison with the nominal 10 wt% WO_3, but σ was relatively low. These data clearly indicate that in the catalysts prepared at pH 2.7 and 5.6 tungsten was preferentially located at the external surface of the USY zeolite, and inhomogeneously distributed. Whereas in the catalyst prepared at pH 11 only a minor amount of W (ca. 13%) was in the outer surface and evenly dispersed, the majority of W may be inside the zeolite particles, probably in the supercages as the sorption data also suggest, since it was undetected by EDX. A similar observation using EDX has also been made previously for zeolite Y extrudates impregnated with ammonium metatungstate (AMT) at different pH (*6*).

The reason for this difference in W location lies fundamentally in the known control exerted by pH on the size of the tungstate species in solution (*27, 28*), as previously suggested (*6, 29*). At pH <7 the AMT contains predominantly polymeric species such $W_{12}O_{39}^{6-}$. These species are too large (ca. 20 Å) to enter the supercages of Y-type zeolite (13 Å), and, therefore, they will remain (adsorbed and/or deposited) on the external surface after impregnation and drying. On the contrary, at pH >7 the dominant monomeric WO_4^{2-} species are able to enter, to some extent, the supercages of the USY zeolite, causing then a reduction in the micropore volume as measured by the N_2 adsorption isotherm.

In line with this, the amount of WO_3 extracted by basic leaching was found to be higher for the W-2.7(550) catalyst (ca. 51%) than for the W-11(550) catalyst (ca. 31%), indicating that W might be more accessible and weakly bound to the zeolite in the former catalyst than in the latter one. These differences in leachable W reflect the differences in W distribution and location among the catalysts.

Effect of Tungsten Incorporation on Surface Acidity

Table 5 lists total acid site concentration and acid strength of both oxided and sulfided states of the W-loaded catalysts calcined at 550°C, and for the calcined USY and USY-11 reference samples. The total acidity of the W-11(550) catalyst was practically equal to the extremely low one of the alkali-treated USY zeolite. Therefore, the increased acidity of the W-5.6(550) and W-2.7(550) catalysts cannot be associated with the incorporation of oxotungsten species. The new acid sites may be hydroxyl groups of the zeolite, formed during the impregnation at acid pH by incorporation of protons. Furthermore, according to the initial electrode potential (Table 5) the acid sites on the W-2.7(550) and W-5.6(550) catalysts are much stronger than those on the USY zeolite.

Upon sulfidation an increased acid site density and comparable acid strength resulted for the W-2.7(550) and W-5.6(550) catalysts, while for the W.11(550) catalyst

TABLE 5

Surface Acidity of Catalysts

Catalyst	Total acidity (meq. *n*-butylamine g^{-1})		Acid strength[a]
	Oxided	Sulfided	Sulfided
USY zeolite	1.32	3.86	v.s.
USY-11	<0.1	—	—
W-2.7(550)	2.19	5.51	v.s.
W-5.6(550)	1.67	4.88	v.s.
W-11(550)	<0.1	<0.1	v.w.

[a] v.s. = very strong acid sites; v.w. = very weak acid sites.

no variation was detected. This increase in catalyst acidity upon sulfidation, also previously observed in NiNaY catalysts (*30*), can be attributed, to some extent, to the dissociative adsorption of H_2S on certain sites of the zeolite lattice. It was suggested that this dissociative H_2S adsorption over NaY zeolites involves certain Na^+ cations at the walls of the supercages (*31*). A similar mechanism involving Ni^{2+} cations was also proposed for sulfided NiNaY zeolites (*30*). In the present case, it is tentatively suggested that the heterolytic dissociation of H_2S could also proceed on other cations such as the cationic aluminum species present in the W-2.7(550) and W-5.6(550) catalysts. This dissociation was not observed on the W-11(550) catalyst, possibly due to the realumination which occurred in such catalyst.

Effect of Tungsten Incorporation on Catalytic Activity

The variation with time-on-stream of thiophene conversion on sulfided samples of 550°C-calcined W-loaded catalysts, and on other reference catalysts, is shown in Fig. 6. On most catalysts the activity decreased very rapidly. Similar activity decays were observed with non-sulfided or calcined samples, and also on the W-loaded catalysts calcined at 450°C, as Fig. 7 illustrates. Deactivation by coking, with a mass balance initially very low (30–58%) and after 3 h time-on-stream close to 100%, was a common feature of all the catalysts studied. However, the relative decay appears to be higher for the USY zeolite and its mechanical mixture with WO_3, the W-11 catalysts, and for calcined samples; in these catalysts the activity drops 95–100% over 2.5 h, whereas for the W-2.7 and W-5.6 catalysts it only decreased 75–85% over the same time period. Such differences in deactivation rate are associated with the nature of the active sites present in the catalysts and of the reaction products, as described below.

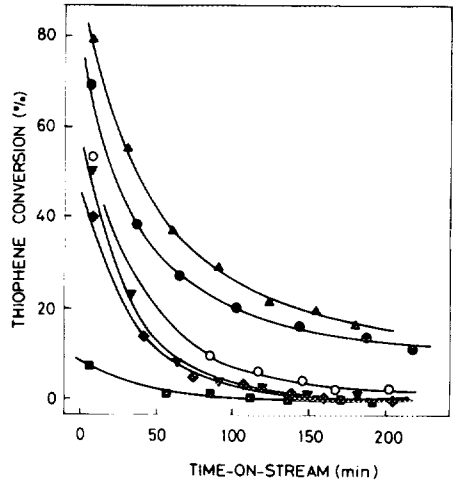

FIG. 6. Conversion of thiophene at 350°C on sulfided catalysts: (▲) W-2.7(550), (●) W-5.6(550), (▼) W-2.7(550)-E, (■) W-11(550), (◆) USY, and (○) mechanical mixture USY + 10 wt% WO_3.

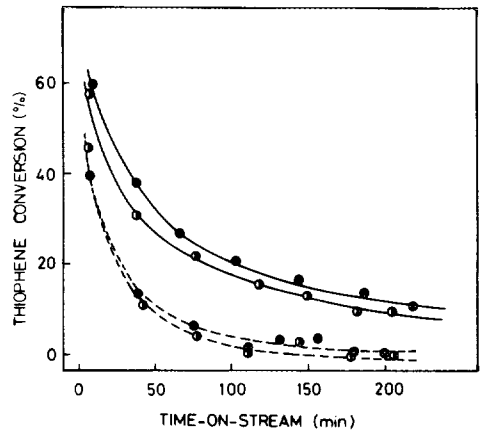

FIG. 7. Conversion of thiophene at 350°C on the catalysts (◑) W-5.6(450), and (●) W-5.6(550) in (---) calcined and (——) sulfided state.

Significant changes in product selectivity were observed among the catalysts. Table 6 shows the product distribution for the 550°C-calcined catalyst samples. Thus for the W-2.7 and W-5.6 catalysts, the major products were butenes (1- and 2-butenes, and butadiene) and *n*-butane, accompanied initially by minor amounts of propylene and/or traces of lighter hydrocarbons (C_1 and C_2). These cracking products, more abundant for the W-2.7 catalysts, practically dis-

TABLE 6

Conversion for the Hydrodesulfurization of Thiophene and Product Distribution at 350°C over Sulfided Catalysts

Catalyst	Time on stream (min)	Conversion (%)	Product distribution (mol%)					
			Butadiene	2-Butene	1-Butene	*n*-Butane	Propylene	$C_1 + C_2$
W-2.7(550)	9	79.7	+	26.6	—	53.8	9.7	+
	181	16.2	10.9	42.7	16.8	29.3	+	+
W-5.6(550)	8	59	1.2	42.8	4.7	42.8	8.2	+
	188	14	16.7	53.4	13.6	16.1	+	+
W-11(550)	8	6.7	—	—	—	—	—	100
	170	<0.1	—	—	—	—	—	100
USY	10	41.6	—	—	—	100	+	+
	203	0.3	+	++	—	—	—	+
(USY + WO_3)[a]	9	53.5	—	26.2	—	73.5	+	++
	182	3.1	+	100	—	+	+	+

Note. +, Traces.
[a] Mechanical mixture containing 10 wt% WO_3.

appeared after ca. 30 min reaction time, suggesting a rapid poisoning through coking of acidic sites. In contrast, on the W-11 catalysts, irrespective of the pretreatment temperature and state, practically only light hydrocarbons (C_1 or C_2) were detected, indicating that the reaction is predominantly cracking via a radical mechanism, as is usual on alkaline-exchanged zeolites (*32*).

The activities of calcined and/or sulfided catalysts for thiophene HDS and subsequent butenes HYD after 8 and 15 min of reaction time are given in Table 7. These values were obtained from the plot of k at different reaction times. It is first noted that the initial HDS activity of the sulfided USY zeolite, a relatively acid catalyst, is about seven times higher than for the sulfided

TABLE 7

Catalytic Activity for Thiophene Hydrodesulfurization (HDS) and Subsequent Butene Hydrogenation (HYD)

Catalyst	Calcined[a]	Sulfided			
	k_{HDS}[b] × 10^6	k_{HDS}[b] × 10^6		k_{HYD}[b] × 10^6	
	t[c] = 8	t[c] = 8	t[c] = 150	t[c] = 8	t[c] = 150
W-2.7(550)	2.00	5.10	0.72	1.92	1.25
W-2.7(550)-E	—	2.73	0.07	~1.00	0.00
W-2.7(450)	2.47	3.26	0.50	1.76	0.69
W-5.6(550)	1.59	2.78	0.60	1.69	0.65
W-5.6(450)	1.75	2.30	0.42	1.85	0.60
W-11(550)	0.23	0.22	~0.00	0.00	0.00
W-11(450)	~0.00	0.19	~0.00	0.00	0.00
USY	1.50	1.80	~0.02	+	+
USY-11	—	0.26	~0.02	+	+
(USY + WO_3)[d]	—	2.50	0.13	~1.2	+

Note. +, Traces.
[a] For this state HYD activity was not appreciable.
[b] Rate constant expressed in mol g^{-1} min^{-1}.
[c] Reaction time in min.
[d] Mechanical mixture containing 10 wt% WO_3.

USY-11, a catalyst with practically no acidity; and that after ca. 2 h of time-on-stream both catalysts have approximately equal very low activity. In addition, it is observed that the sulfided USY zeolite was slightly more reactive than its calcined form and, on the other hand, the acidity of the former catalyst was clearly higher than that of the latter, but both behaved similarly with time on stream. All these results confirm early findings (*8*), that the strong Brønsted acidic sites present on zeolites catalyze the hydrogenolysis of thiophene; however, such sites are rapidly deactivated by coking caused by butenes and propylene, the major products initially formed on these catalysts. The absence of a hydrogenation function in the USY zeolite is reflected by the non-detection of *n*-butane in the reaction products, except for times on stream <8 min.

The addition by mechanical mixing of WO_3 to the USY led to a substantial increase in HDS activity at the initiation of the reaction and after about 2 h of reaction, besides a small HYD activity as revealed by the presence of minor amounts (initially) or traces (for $t > 8$ min.) of *n*-butane. Such HYD activity is due evidently to the sulfided WO_3 species.

Comparing the HDS activities of all the sulfided W-loaded zeolite catalysts, it is clearly seen that initially, as well as in the long term, the highest HDS and HYD activity was found for the catalysts prepared at pH = 2.7, which exhibited significantly higher acidity (Table 5), and which had the major fraction of tungsten on the external surface of the zeolite according to the above characterization results. Similarly, the W-loaded catalysts prepared at pH = 5.6, with almost the same amount of tungsten on the external surface and slightly minor acidity than the W-2.7(550) catalyst, presented moderate activity for both HDS and HYD reactions. Furthermore, in both catalysts the HYD activity was measurable during all the reaction time, and the values differed only slightly. Another interesting result is that the removal of about 51% of W from the W-2.7(550) catalyst, viz., the W.2.7(550)-E catalyst, caused the disappearance of cracking products, a decrease (~50%) in HDS activity and shorter lifetime due to a fast deactivation of the remaining acidic active sites. In contrast to the W-2.7 catalysts, the non-acidic W-11 catalysts, which contain most of the tungsten inside the zeolite, exhibited only initially a small HDS activity (about 25 times lower than for the W-2.7(550) catalyst), no HYD activity, and short lifetime. Nevertheless, it is noted that the HDS activities of the sulfided catalysts do not keep a direct correlation with their acidities. We consider that the increased HDS activity of the W-2.7 and W-5.6 catalysts, in comparison with the parent USY zeolite, is associated with the increased acidity and also with the location of the sulfided (in some extent) tungsten oxide species located mainly outside the zeolite. Full sulfidation of the external tungsten oxide species is not likely to occur due to the low sulfidability of the alumina-supported WO_3 catalysts (*33*).

The catalytic contribution of the sulfided W species to the overall reaction, revealed also by the appearance of a substantial and steady HYD, may increase with reaction time because such species deactivated less rapidly and to a smaller extent than the acidic sites, leading to an increase in the HYD selectivity with time-on-stream. Indeed, this effect on selectivity is clearly shown in Fig. 8; at about 2 h of reaction time the highest k_{HYD}/k_{HDS} ratio is shown by the W-2.7(550) catalyst, which contains more tungsten outside the zeolite. On such external sulfided tungsten species the reaction may continue after the inside active sites are deactivated and/or blocked.

The fact that the W-11 catalysts showed very low HDS activity suggests that either tungstate located in the supercages may not be readily sulfided or that the resulting highly disperse sulfided W species become rapidly blocked by coke formation, besides a much more limited access of thiophene to

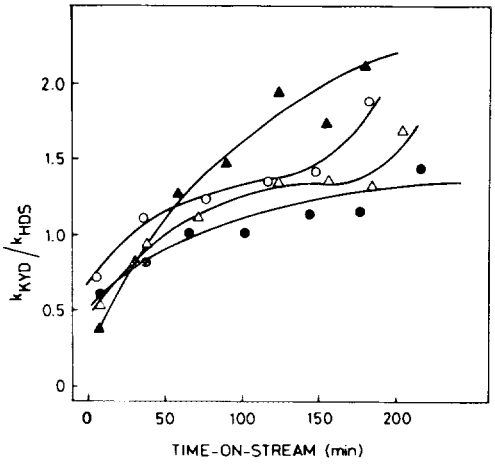

FIG. 8. Ratio between the reaction rate constants for butene HYD and thiophene HDS at 350°C as a function of time-on-stream for catalysts (▲) W-2.7(550), (△) W-2.7(450), (●) W-5.6(550), and (○) W-5.6(450).

the active sites, as also suggested elsewhere in connection with $Mo(CO)_6$-loaded Y-zeolite catalysts (*20*). Data on sulfidation of the W oxide species deposited inside zeolite cavities are not available. However, for similar Mo species located inside HY zeolites it was shown (*34*) that in most cases sulfidation of Mo was incomplete; full sulfidation was obtained only when the Mo content was very low. Considering that the sulfidability of W oxide species is much lower than those of Mo, it seems probable that very little of the internal W oxide species can be sulfided. Nevertheless, from the present characterizaton results none of these possibilities can be excluded.

Regarding the non-presulfided catalysts, Table 7 shows that the general order of activity was similar to that for the sulfided ones, but the differences in HDS activity among the former were smaller than for the sulfided catalysts. The absence of sulfided tungsten species, at least initially, may reduce considerably their catalytic contribution to the overall reaction, especially for the W-2.7 and W-5.6 catalysts. In this case, catalyst reactivity is predominantly due to the acid sites which deactivate rapidly; consequently, *n*-butane was generally not observed in the reaction products. In accordance with the minor acidity of the non-presulfided catalysts, with them cracking products appeared only as traces.

CONCLUSIONS

In the preparation of W-loaded (10 wt% WO_3) ultrastable Y zeolite catalysts prepared by impregnation with excess solution containing ammonium *meta*-tungstate, the pH of the impregnation solution controls the distribution of tungsten in the final calcined catalyst. In acid preparations (pH ~2.7), as large polytungstate anions predominate in solution, the majority of the tungsten is relatively well dispersed on the external surface of the zeolite, and also catalyst acidity is considerably increased, especially after the sulfidation with H_2S. These two factors increase the cracking and HDS activities of the ultrastable zeolite, provide an additional HYD activity, and apparently reduce its deactivation.

However, at pH close to 11, conditions in which the WO_4^{2-} species predominate, a substantial part of tungsten is inside the zeolite supercages. This location of tungsten, in conjunction with the resultant loss of catalyst acidity, considerably decreases the initial HDS activity of the USY zeolite and its lifetime, and practically does not add any HYD activity.

Under the conditions used, the incorporation of tungsten to the zeolite produces only minimal or moderate loss in zeolite crystallinity, depending on the impregnation pH being basic or acid. This effect is accompanied by some realumination of the zeolite for the catalysts impregnated at pH 11, due to its adjustment with NaOH solution, and conversely, by a small dealumination for the catalysts impregnated at pH 2.7.

ACKNOWLEDGMENTS

We are grateful to the DGICYT (Spain) Projet PB87-0261, Dirección de Investigación de la Universidad de Concepción (Chile), OEA, and the Program of Scientific Cooperation between CSIC (Spain) and CONICYT (Chile), for financial support.

REFERENCES

1. Streed, C. W. and Yan, T. Y., U.S. Patent 3.702.818 (1972).
2. Hoepfner, E., Schuetter, H., Franke, H., Limmer, H., Hergeth, H., Dochler, E., Goltz, N., Bohlman, D., Matthey, R., *et al.* (VEB Petrolchemishes Kombinat Schwedt), Ger (East) Patent DD 262,443 (1989).
3. Miller, J. T., U.S. Patent 4,812,224 (1989).
4. Yan, Y. T., *Ind. Eng. Chem. Process Des. Dev.* **22,** 154 (1983); **28,** 1463 (1989).
5. Chan-yu, Y., Hatcher, W. J., Jr., and Wolfgang, B., *Ind. Eng. Chem. Res.* **28,** 13 (1989).
6. Hutchings, G. J., and Buckles, G., *in* "Proceedings of the 8th International Zeolite Conference, July 1989, Amsterdam; Zeolites: Facts, Figures, Future" (P. A. Jacobs and R. A. van Santen, Eds.), Studies in Surface Science and Catalysis, Vol. 49B, p. 1413. Elsevier, Amsterdam, 1989.
7. Cid, R., Gil Llambias, F. J., Fierro, J. L. G., López Agudo, A., and Villaseñor, J., *J. Catal.* **89,** 478 (1984).
8. López Agudo, A., Cid, R., Orellana, F., and Fierro, J. L. G., *Polyhedron* **5,** 187 (1986).
9. Fierro, J. L. G., Conesa, J. C., and López Agudo, A., *J. Catal.* **108,** 334 (1987).
10. Jacobs, P. A., Derouane, E. G., and Weitkamp, J., *J. Chem. Soc. Chem. Commun.*, 591 (1981); Coudurier, G., Naccache, C. and Védrine, J. C., *J. Chem. Soc. Chem. Commun.*, 1415 (1982); Kultarni, S. B., Shiralkar, V. P., Kolasthane, A. N., Borade, R. B., and Ratnasamy, P., *Zeolites* **12,** 313 (1982).
11. Cid, R., and Pechi, G., *Appl. Catal.* **14,** 15 (1985).
12. Okamoto, Y., Tomioka, H., Imanaka, T., and Teranishi, S., *J. Catal.* **66,** 93 (1980).
13. Scherzer, J., *J. Catal.* **54,** 285 (1978).
14. Beyer, H. K., Belenykaja, I. M., Hange, F., Tielen, M., Grobet, P. J., and Jacobs, P. A., *J. Chem. Soc. Faraday Trans. 1* **81,** 2889 (1985).
15. Breck, D. W. and Skeels, G. W., *in* "Proceedings of the 5th International Conference on Zeolites" (L. V. C. Rees, Ed.), p. 335. Heyden, London, 1980.
16. Ceranic, T. S., Radak, V. M., Lukic, T. M. and Nikolic, D., *Zeolites* **5,** 42 (1985).
17. Handan, H., Sulikowski, B. and Klinowski, J., *J. Phys. Chem.* **93,** 350 (1986).
18. Klinowski, J., Hamdan, H., Corma, A., Fornés, V., Hunger, M., and Freude, D., *Catal. Lett.* **3,** 263 (1989).
19. Flanigen, E. M., Khatami, H. and Szymanski, H. A., *in* "Molecular Sieve Zeolites I" (E. M. Flanigen and L. B. Sand, Eds.) Adv. Chem. Ser. No. 101, p. 201. American Chemical Society, Washington, DC, 1971.
20. Laniecki, M., and Zmierczak, W., *Zeolites* **11,** 18 (1991).
21. Yon-Sing, Y., and Howe, R. F., J. Chem. Soc., *Faraday Trans. 1* **82,** 2887 (1986).
22. Maugé, F., Courcelle, J. C., Engelhard, Ph., Gallezot, P., Grosmangin, J., Primet, M., and Trusson, B., *in* "Zeolites" (B. Drzaj, S. Hočevar, and S. Pejovnik, Eds.) p. 401. Elsevier, Amsterdam, 1985.
23. Lohse, V., Stach, H., Thamm, H., Schirmer, W., Isirikjan, A. A., Regent, N. I., and Dubinin, M. M., *Z. Anorg. Allg. Chem.* **460,** 179 (1980).
24. Lynch, J., Raatz, F. and Dufresne, P., *Zeolites*, **7,** 333 (1987).
25. Sing, K. S. W., *Pure Appl. Chem.* **54,** 2201 (1982).
26. Barrett, E. P., Joyner, L. G., and Halenda, P. H., *J. Am. Chem. Soc.* **73,** 373 (1951).
27. Kepert, D. L., *Prog. Inorg. Chem.* **4,** 199 (1962).
28. Tytko, K-H., and Glemser, O., *Adv. Inorg. Chem. Radiochem.* **19,** 239 (1976).
29. Maitra, A. M., Cant, N. W., and Trimm, D. L., *Appl. Catal.* **27,** 9 (1986).
30. Cid, R., Fierro, J. L. G., and López-Agudo, A., *Zeolites* **10,** 95 (1990).
31. Karge, H. G. and Rasko, J., *J. Colloid Interface Sci.* **64,** 522 (1978).
32. Poutsma, M. L., and Schaffer, S. R., *J. Phys. Chem.* **77,** 158 (1973).
33. Scheffer, B., Mangnus, P. J., and Moulijn, J. A., *J. Catal.* **121,** 18 (1990).
34. Ezzamarty, A., Catherine, E., Cornet, D., Hémidy, J. F., Janin, A., Lavalley, J. C., Leglise, J. and Mériaudeau, P., *in* "Zeolites: Facts, Figures, Future" (P. A. Jacobs and R. A. van Santen, Eds.), Studies in Surface Science and Catalysis, Vol. 49B, p. 1025. Elsevier, Amsterdam, 1989.